International Journal of Biochemistry and Cell Biology 95 (2018) 27–34

Contents lists available at ScienceDirect

International Journal of Biochemistry and Cell Biology

journal homepage: www.elsevier.com/locate/biocel

Silica nanoparticle releases SIRT6-induced epigenetic silencing of follistatin

Lingda Zhang[1], Bing Han[1], Jie Xiang, Kangli Liu, Haojie Dong, Xiangwei Gao*

Institute of Environmental Medicine, Zhejiang University School of Medicine, Hangzhou, China

ARTICLE INFO

Keywords:
SIRT6
Follistatin
Transcription
Silica nanoparticle
Apoptosis

ABSTRACT

Follistatin (FST) plays a protective role during silica nanoparticle (SiO_2 NP) exposure. SiO_2 NP treatment induces FST transcription with an unknown mechanism. We herein reported that SIRT6, one of the sirtuin family members, induced epigenetic silencing of FST. The expression of FST was elevated after SIRT6 knockdown while reduced after SIRT6 overexpression. Chromatin immunoprecipitation revealed a direct interaction between SIRT6 with FST promoter. Knockdown of SIRT6 increased both Ac-H3K9 level and Ac-H3K56 level at FST promoter region. SiO_2 NP treatment de-stabilized SIRT6 mRNA and reduced SIRT6 expression, leading to the activation of FST transcription. Finally, over-expression of SIRT6 increased SiO_2 NP-induced apoptosis. Collectively, this study provided evidence that SIRT6 is a negative regulator of FST transcription and participates in the regulation of cell survival during silica nanoparticle exposure.

1. Introduction

Nanoparticles (NPs) are engineered structures with less than 100 nanometers in at least one dimension, among which silica nanoparticle (SiO_2 NP) is one of the most widely applied (Li et al., 2012; Nel et al., 2006). The wide use of SiO_2 NP has raised serious concerns about their safety for human health. The respiratory system is one of the main routes by which SiO_2 NPs access human body (Nel et al., 2006; Nel et al., 2009; Oberdorster, 2010). SiO_2 NP exposure induces the generation of reactive oxygen species (ROS) in airway epithelial cells and macrophages, which damages cellular proteins, lipids, and DNA (Brown et al., 2014; Nel et al., 2006). The elevated ROS triggers cellular oxidative stress responses which finally induce the expression of protective proteins including antioxidant enzymes, detoxification enzymes, and stress-response proteins (Ma, 2013). These SiO_2 NP-responsive proteins exert antioxidant and cytoprotective effects in respiratory system (Ma, 2013; Nel et al., 2006). However, besides a few Nrf2 target genes, the regulation of other SiO_2 NP-responsive genes and their functions in SiO_2 NP response remain to be identified.

Follistatin (FST) is widely expressed in higher animals and participates in a variety of processes such as cell growth, development, differentiation, and secretion (Hemmati-Brivanlou et al., 1994). FST was firstly identified as a secretory protein that binds and inactivates transforming growth factor (TGF)-β family members including activin, bone morphogenetic proteins (BMPs), and myostatin. The TGF-β-like molecule-neutralizing effect of FST contributes to most of its functions (Amthor et al., 2004; Glister et al., 2004; Nakamura et al., 1990). Recent studies showed that FST also plays a protective role under oxidative stress (Lim et al., 2015). It was reported that activin induces endothelial cell oxidative stress and endothelial cell dysfunction, and these effects are mitigated by follistatin (Lim et al., 2015). Follistatin has also been reported to suppress BMP4-induced ROS production (Jiang et al., 2015). We have demonstrated that SiO_2 NP induced the expression of FST in mouse lung tissue as well as in human lung epithelial cells. The elevated FST inhibited SiO_2 NP-induced ROS production and cell apoptosis. Interestingly, the levels of Ac-H3(K9/18), an active gene marker, at FST promoter region was significantly increased during SiO_2 NP treatment, indicating an activation of FST transcription (Lin et al., 2016). However, the detailed mechanism underlying SiO_2 NP-induced FST transcription remains elusive.

Sirtuins are nicotinamide adenine dinucleotide (NAD^+)-dependent deacetylases that regulate lifespan in lower organisms. To date, seven mammalian homologues (SIRT1 ~ SIRT7) have been identified with varied subcellular localizations and enzymatic activities (Michishita et al., 2005). SIRT6, one of the sirtuins, is mainly localized in the nucleus of the cells. It deacetylates histones H3 at either lysine 9 (H3K9) or lysine 56 (H3K56) and represses its target gene expression (Michishita et al., 2008; Michishita et al., 2009; Yang et al., 2009). Through its deacetylation activity, SIRT6 regulates a variety of cellular processes including chromosome stability, inflammation, cell metabolism, apoptosis, and senescence.

Recent studies have shown that SIRT6 participates in cellular response to stresses. In mammalian cells subjected to oxidative stress SIRT6 is recruited to the sites of DNA double-strand breaks (DSBs) and

* Corresponding author at: Institute of Environmental Medicine, Zhejiang University School of Medicine, 866 Yuhangtang Road, Hangzhou 310058, China.
E-mail address: xiangweigao@zju.edu.cn (X. Gao).
[1] These authors contributed equally to the work.

https://doi.org/10.1016/j.biocel.2017.12.011
Received 11 September 2017; Received in revised form 29 November 2017; Accepted 11 December 2017
Available online 12 December 2017

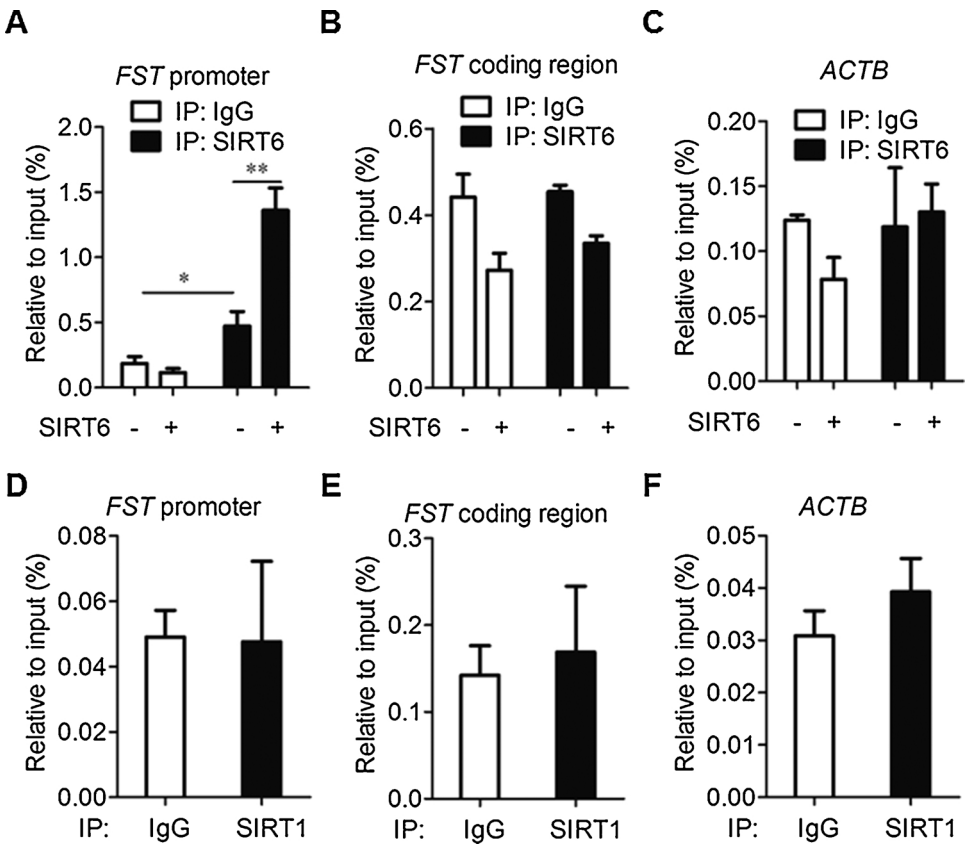

Fig. 1. SIRT6 binds to the promoter region of FST. (A,B,C) A549 cells infected with virus expressing SIRT6 or control vector. ChIP analysis was performed with antibodies against SIRT6 or control IgG and analyzed by qPCR. The occupancies of SIRT6 at FST promoter region (A), FST coding region (B), or ACTB gene (C) were normalized to the input DNA. The values are the mean ± SD of three independent experiments. $^{**}P < 0.01$. (D,E,F) ChIP analysis was performed with antibodies against SIRT1 or control IgG and analyzed by qPCR. The occupancies of SIRT1 at FST promoter region (D), FST coding region (E), or ACTB gene (F) were normalized to the input DNA.

stimulates DSB repair, through both nonhomologous end joining and homologous recombination (Mao et al., 2011). Knockout of SIRT6 in human mesenchymal stem cells (hMSCs) showed dysregulated redox metabolism and increased sensitivity to the oxidative stress. The function of SIRT6 in maintaining hMSC homeostasis relies on its interaction with Nrf2 and transactivation of NRF2-regulated antioxidant genes (Pan et al., 2016). SIRT6 is also involved in camptothecin-induced DNA damage response. Knockdown of SIRT6 up-regulates TRF2 protein levels and counteracts its down-regulation during DNA damage response, leading to cell survival (Rizzo et al., 2017). However, the function of SIRT6 under SiO_2 NP stress remains unidentified.

In this study, we evaluated the regulation of SIRT6 on FST expression and its role under SiO_2 NP stress. We found that SIRT6 negatively regulates FST through deacetylation of H3K9 and H3K56 at FST promoter. SiO_2 NP decreased SIRT6 expression, which accounts for the up-regulated FST level.

2. Materials and methods

2.1. Silica nanoparticles

SiO_2 nanoparticle was from Sigma-Aldrich (Sigma-Aldrich, St. Louis, MO, United States). Nanoparticles were dispersed in double distilled water at the concentration of 10 mg/mL. Nanoparticles were sonicated at 200 W for 30 s prior to cell or mouse treatment.

2.2. Cells culture and nanoparticle treatment

Lung epithelial cells (A549) were obtained from ATCC and cultured in RPMI-1640 medium supplemented with 10% fetal bovine serum (Thermo Fisher Scientific, Waltham, MA, United States). Cells were maintained at 37 °C in an atmosphere containing 5% CO_2 and 100% humidity.

For SiO_2 NP treatment, cells were seeded in 6-well plates. After 24 h, cells were treated with silica nanoparticles suspended in RPMI-1640 supplemented with 1% fetal bovine serum at different concentration for indicated time and then subjected to further experiments.

2.3. Plasmids

For the construction of SIRT6 expressing lentiviral plasmid, SIRT6 coding region was amplified by PCR and cloned to vector pCDH between *Eco*RI and *Bam*HI sites.

For the construction of SIRT6 promoter plasmid, SIRT6 promoter region was amplified by PCR and cloned to vector pGL3-basic between *Xho*I and *Hind*III sites.

For the construction of shRNA plasmid targeting SIRT6, lentviral vector pLKO was used. shRNA oligonucleotides were designed using sigma online protocol. Synthesized DNA oligos were annealed and ligated into the *Age*I/*Eco*RI-digested pLKO vector.

All the oligo sequences were listed in supplemental Table 1.

2.4. shRNA lentivirus production

To produce lentivirus expressing SIRT6/SIRT6-shRNA, the plasmid pCDH-SIRT6/pLKO-shSIRT6, the envelope plasmid pMD2G and the packaging plasmid psPAX2 were co-transfected into 293T cells. Lentiviral supernatants were harvested through a 0.45 μm filter 48 h after transfection.

2.5. RNA purification and reverse transcription reaction

Total RNA was isolated with Trizol reagent (Thermo Fisher Scientific) following the manufacturer's protocol. 0.5 μg of total RNA was reverse transcribed using random hexamers and the High Capacity cDNA Reverse Transcription Kit (Thermo Fisher Scientific).

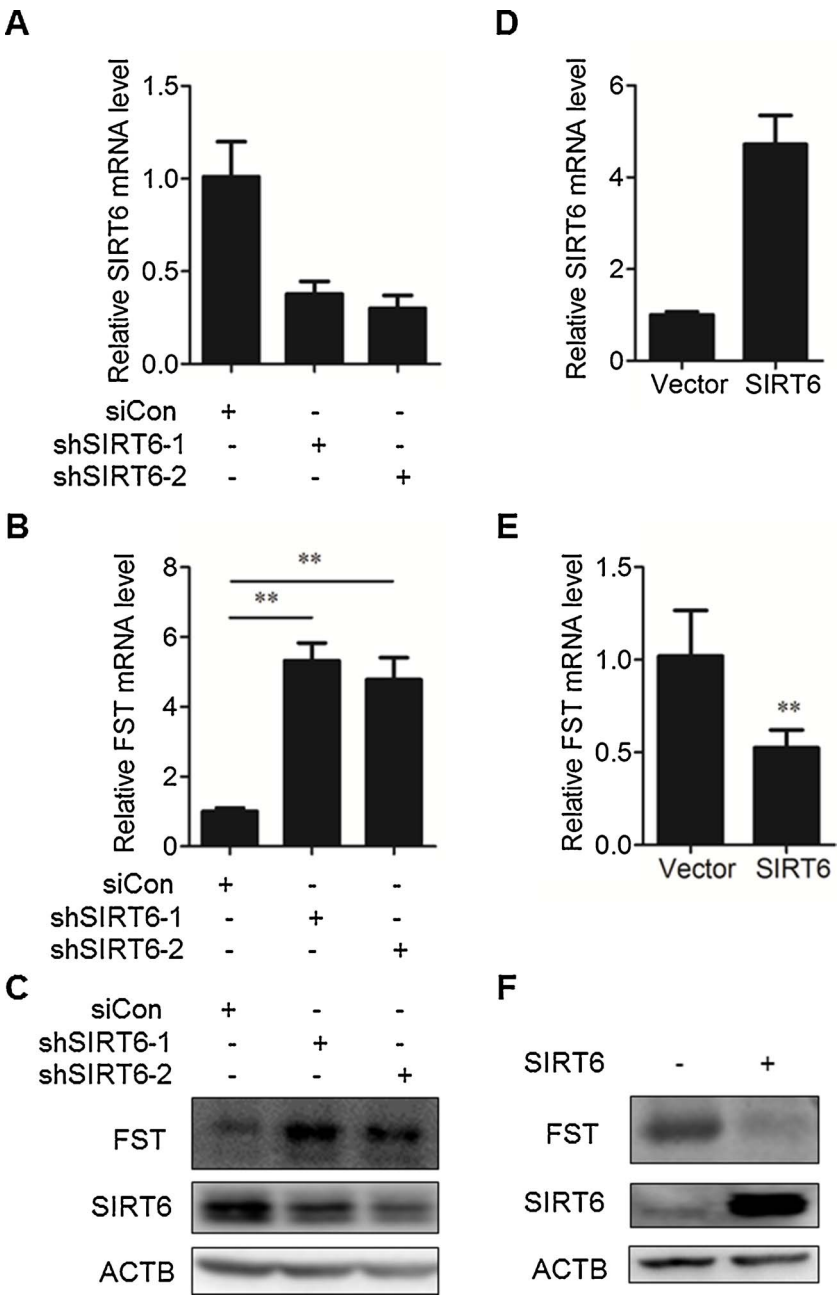

Fig. 2. SIRT6 inhibits FST expression.
(A,B,C) A549 cells were infected with virus expressing shRNA targeting SIRT6 or control shRNA. The mRNA level of SIRT6 (A) and FST (B) was detected by qPCR. (C) The protein level of FST and SIRT6 was detected by immunoblotting. (D,E,F) A549 cells were infected with virus expressing SIRT6 or control vector. The mRNA level of SIRT6 (D) and FST (E) was detected by qPCR. (F) The protein level of FST and SIRT6 was detected by immunoblotting.

2.6. Real-time quantitative PCR analysis

Real-time quantitative PCR analysis was performed in 10-μl reactions using SYBR GREEN PCR Master Mix (Thermo Fisher Scientific). The related mRNA level was normalized to the *β-actin* mRNA level. Data were analyzed using the $2^{-D\Delta Ct}$ method (Livak and Schmittgen, 2001). Sequences of all the primers used for PCR amplification are listed in supplemental Table 1.

2.7. Immunoblotting analysis

Proteins were quantified by BCA protein assay kit (Bio-Rad) and applied to immunoblotting analysis as described previously [2]. 50 μg of total proteins were subjected to sodium dodecylsulfate polyacrylamide gel electrophoresis (SDS-PAGE) and transferred to nitrocellulose membrane (Whatman, Clifton, NJ, United States). Membrane was blocked with 3% bovine serum albumin (BSA) TBS-T buffer (20 mM Tris-HCl, pH 8.0, 150 mM NaCl, 0.05% Tween- 20), probed with antibodies targeting to FST (Santa Cruz Biotechnology, Santa Cruz, CA, United States), SIRT6 (Abcam, Cambridge, MA, United States) or ACTB (Cell Signaling Technology, Beverly, MA, United States). Membrane was incubated with horseradish-conjugated secondary antibodies, detected with the SuperSignal West Pico chemiluminescence substrate (Thermo Fisher Scientific), and finally exposed to an X-ray film.

2.8. Chromatin immunoprecipitation (ChIP)

ChIP assays were performed using the ChIP assay kit (Thermo Fisher Scientific) following the manufacturer's protocol. Briefly, A549 cells were cross-linked with 1% formaldehyde for 10 min at 37 °C. Cross-linking was stopped with 0.125 M glycine. After sonication to yield DNA fragments of 300–1000 base pairs, the lysates were cleared by centrifugation, diluted 6-fold with ChIP dilution buffer, and precleared with salmon sperm DNA/protein A-agarose at 4 °C for 1 h. For each immunoprecipitation assay, the lysates were incubated with 2 μg of

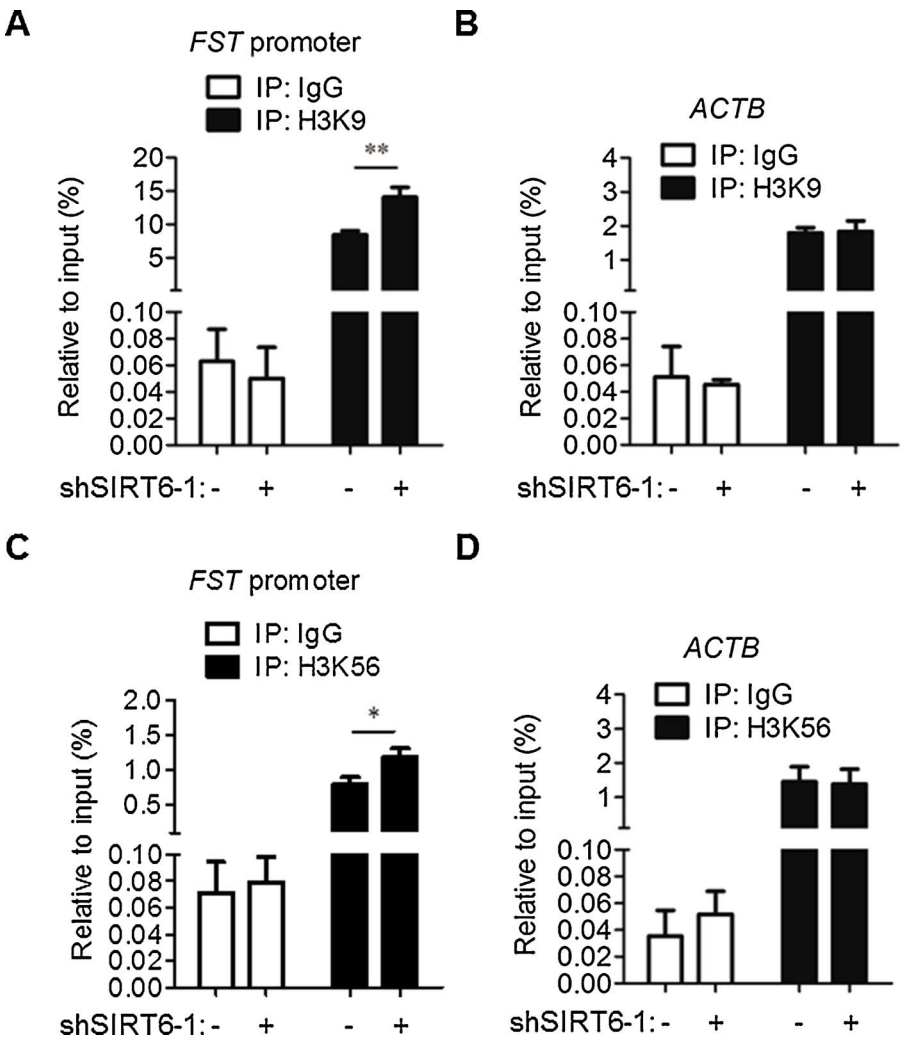

Fig. 3. SIRT6 reduces Ac-H3K9 and Ac-H3K56 levels at FST promoter region.
A549 cells were infected with virus experssing shRNA targeting SIRT6 or control shRNA. ChIP analysis was performed with antibodies against Ac-H3K9, Ac-H3K56 or control IgG and analyzed by qPCR. The occupancies of Ac-H3K9 (A) and Ac-H3K56 (C) at FST promoter region were normalized to the input DNA. The occupancies of Ac-H3K9 (B) and Ac-H3K56 (D) at ACTB gene were used as control. The values are the mean ± SD of three independent experiments. $^{**}P < 0.01$.

anti-SIRT6 (Abcam), anti-SIRT1 (Millipore), anti-acetylated histone H3 (Lys9) (Ac-H3, K9) (Thermo Fisher Scientific), anti-acetylated histone H3 (Lys56) (Ac-H3, K56) (Abclonal, Wuhan, China) or control IgGs (Santa Cruz Biotechnology) overnight at 4 °C with rotation. The immunocomplexes were then collected with protein A-agarose slurry, eluted, and de-crosslinked at 65 °C. After RNase digestion and proteinase digestion, immunoprecipitated DNA was extracted. The purified DNA was amplified by real time qPCR.

Sequences of the primers used for FST promoter amplification are listed in supplemental Table 1.

2.9. Luciferase assay

A549 cells were transfected with SIRT6 promoter and pRL-TK was co-transfected as the internal control. 24 h after transfection, cells were treated with SiO_2 NPs for another 12 h. Cells were then lysed and luciferase activity was measured by the Dual-Luciferase assay system (Promega, Madison, WI, United States). The firefly luciferase activity was normalized to renilla luciferase.

2.10. ROS detection

Total ROS was detected by using a fluorescent probe 2′,7′-dichlorofluorescin-diacetate (DCFH-DA) (Beyotime, Nanjing, China). Briefly, cultured A549 cells were treated with or without SiO_2 NPs for 2 h and then incubated with 10 μM of DCFH-DA at 37 °C for 30 min. After rinsing with PBS to eliminate excess DCFH-DA, cells were harvested in 0.5 ml PBS and the fluorescence intensity was monitored with flow cytometry (FCM).

2.11. CCK8-based viability assay

The effect of SiO_2 NP on cell viability was assessed by Cell Counting Kit-8 (CCK8) assay (Dojindo Laboratory, Japan). Cells were then treated with SiO_2 NPs for another 12 h. 10 μl of CCK8 reagent was added to each well and the cells were incubated for 2 h at 37 °C. The optical density (OD) at 450 nm was measured by using *Varioskan*Flash (Thermo Scientific).

2.12. Apoptosis assay

After SiO_2 NP treatment for 12 h, both floating and attached cells were harvested and applied to annexin V detection. Briefly, resuspended cells were stained with 5 μl of annexin V-FITC/PI (Biovision, Mountain View, CA, United States) for 5 min in the dark and then analyzed by flow cytometry (Beckman Coulter, Brea, CA, United States).

2.13. Statistical analysis

The experiments were repeated at least three times and data were presented as mean ± SD. Statistical significance between two groups was determined with the Student's *t*-test. All comparisons were two-tailed and $P < 0.05$ was considered significant.

3. Results

3.1. SIRT6 binds to the promoter region of FST

We have previously reported that SiO_2 NP induced the transcription of FST. Moreover, SiO_2 NP increased the level of Ac-H3(K9/18) at FST promoter region, indicating that SiO_2 NP induces FST expression through an epigenetic mechanism (Lin et al., 2016). Sirtuins are NAD^+-dependent deacetylases and many of the family members are implicated in cellular stress response. To address which of sirtuins regulates FST transcription, we transfected cells with siRNA targeting SIRT1-7 and examined FST mRNA level. Data showed that down-regulation of SIRT1 and SIRT6 induced a significant increase of FST mRNA (Fig. S1). Both SIRT1 and SIRT6 are nuclear localized and act as a transcriptional co-factors (Michishita et al., 2008; Michishita et al., 2005; Tasselli et al., 2016). To determine whether SIRT1 and SIRT6 regulated FST expression by binding to its promoter, chromatin immunoprecipitation was carried out. The purified SIRT6- or SIRT1-bound DNA sequences from ChIP experiments were then analyzed by qPCR. An enrichment of the sequence located on the FST promoter was detected in anti-SIRT6 group, as compared with IgG group (Fig. 1A). The sequences on FST coding region or ACTB gene was not enriched in anti-SIRT6 group compared to IgG group, indicating the specific binding between SIRT6 with FST promoter (Fig. 1B,C). Expectedly, overexpression of SIRT6 significantly increased the binding of SIRT6 to FST promoter (Fig. 1A). However, we did not detect the binding between SIRT1 and FST promoter (Fig. 1D–F). These data suggested that SIRT6 directly regulates FST transcription while SIRT1 regulates FST expression indirectly. Therefore, we focused on SIRT6 in the following work.

3.2. SIRT6 inhibits FST expression

To further confirm the regulation of FST transcription by SIRT6, we silenced endogenous SIRT6 using shRNAs and detected FST expression. Two shRNAs targeting SIRT6 could efficiently silence SIRT6 expression (Fig. 2A,C). Knockdown of SIRT6 significantly increased both the mRNA and protein level of FST (Fig. 2B,C). Consistently, inhibition of SIRT6 activity with its inhibitor also upregulated FST expression (Fig. S2) (Parenti et al., 2014). Cells over-expressing SIRT6 displayed a marked decrease in FST expression compared with null vector-transfected cells (Fig. 2D–F). These data indicated that FST transcription was indeed repressed by SIRT6 under normal growth condition.

3.3. SIRT6 reduces Ac-H3K9 and Ac-H3K56 levels at FST promoter region

SIRT6 deacetylates histones H3 at either lysine 9 (H3K9) or lysine 56 (H3K56) (Michishita et al., 2008; Michishita et al., 2009; Yang et al., 2009). To determine whether SIRT6 deacetylates histone H3 at FST promoter, we performed ChIP assay to analyze Ac-H3K9 and Ac-H3K56 levels at FST promoter region after silencing SIRT6. Data showed that knockdown of SIRT6 indeed significantly increased both Ac-H3K9 level and Ac-H3K56 level at FST promoter region (Fig. 3A,C). As a negative control, the Ac-H3K9 level and Ac-H3K56 level at ACTB gene did not change after SIRT6 knockdown (Fig. 3B,D). Knockdown of SIRT1 did not affect the Ac-H3K9 level and Ac-H3K56 level at FST promoter (Fig. S3).

3.4. SiO_2 NP treatment decreases SIRT6 expression

The data above indicated SIRT6-induced epigenetic silencing of FST gene under normal growth condition. Since FST expression was induced during SiO_2 NP exposure, we asked whether SIRT6 responds to SiO_2 NP stress. To that end, A549 cells were treated with SiO_2 NP and SIRT6 expression was detected. The mRNA level of SIRT6 started to decrease 1 h after SiO_2 NP treatment, while the protein level started to decrease at 3 h of SiO_2 NP treatment (Fig. 4A,B). Furthermore, we intratracheally instilled mice with SiO_2 NP and detected SIRT6 expression. Data showed that both the mRNA level and the protein level of SIRT6 decreased after 1 day of SiO_2 NP treatment (Fig. 4C,D). Altogether, our results revealed that SiO_2 NP treatment decreases SIRT6 expression.

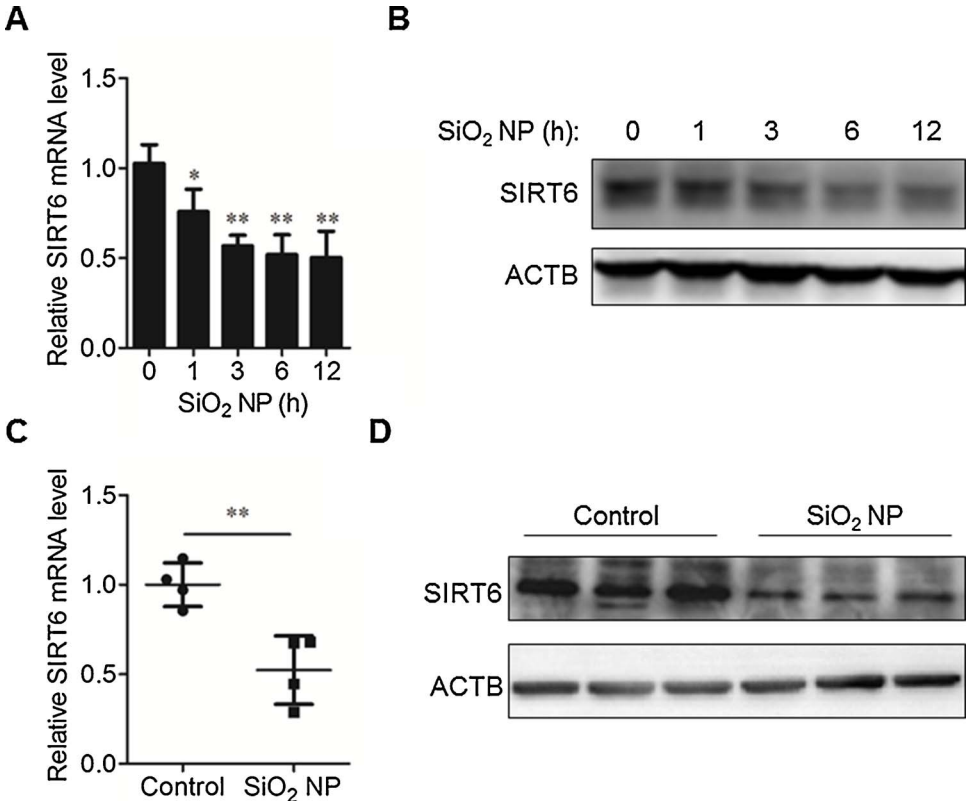

Fig. 4. SiO_2 NP treatment decreases SIRT6 expression.
(A,B) A549 cells were incubated with or without 50 μg/mL of SiO_2 NPs and harvested at the indicated time. (A) The SIRT6 mRNA level was measured by real time qPCR. Data are presented as the mean ± SD of three independent experiments. $^*P < 0.05$, $^{**}P < 0.01$. (B) The SIRT6 protein level was detected by immunoblotting. (C,D) Mouse lung was instilled with PBS or 100 μg of SiO_2 NPs and harvested at the indicated time. (C) The SIRT6 mRNA level in mouse lung tissue was measured by real time qPCR and normalized to *ACTB* mRNA level. $^*P < 0.05$, $^{**}P < 0.01$. (D) The lung tissue protein lysates from paired mice were subjected to immunoblotting for SIRT6 detection.

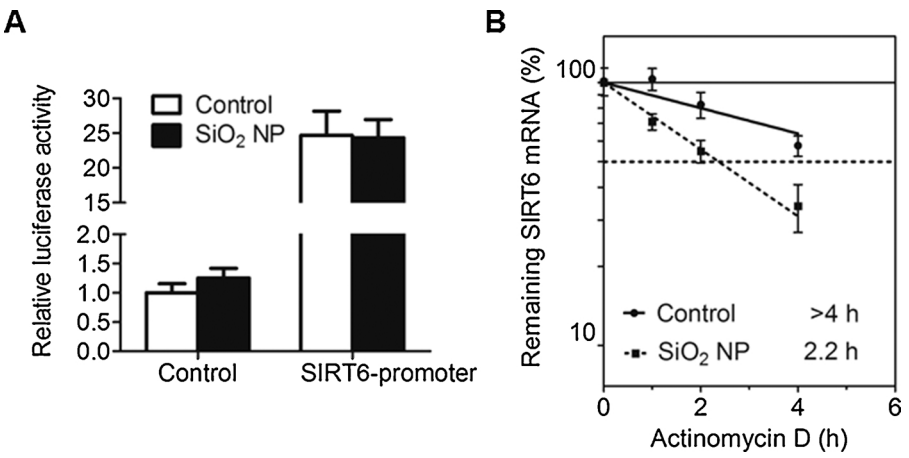

Fig. 5. SiO_2 NP treatment de-stabilizes SIRT6 mRNA.
(A) A549 cells transfected with SIRT6 promoter luciferase reporter and renilla luciferase internal control were treated with or without 50 μg/mL of SiO_2 NPs for 12 h. Luciferase activity was then detected and normalized to renilla activity. (B) A549 cells treated with or without SiO_2 NPs were incubated with 5 μg/mL of actinomycin D for 0, 2, and 4 h. SIRT6 mRNA level was measured and normalized to *ACTB* mRNA level. The half-life of each mRNA is defined as the time needed to reach 50% of its original abundance at time 0 h (dashed line). Data shown are means ± SD of three independent experiments.

3.5. SiO_2 NP treatment de-stabilizes SIRT6 mRNA

The reduced level of SIRT6 mRNA may result from either transcriptional depression or post-transcriptional regulation. We therefore first detected SIRT6 gene promoter activity using a luciferase reporter. Data showed that the transcriptional activity of SIRT6 promoter was not significantly induced under SiO_2 NP treatment (Fig. 5A). Next, we examined the stability of SIRT6 mRNA. Actinomycin D was used to block *de novo* RNA synthesis, and then the persistence of the existing SIRT6 mRNA was measured by qPCR at 0, 2, and 4 h. Our results revealed that SiO_2 NP treatment led to substantial stabilization of the SIRT6 mRNA. The half-life of total SIRT6 mRNA is control cells than SiO_2 NP-treated cells (Fig. 5B, $>$ 4 h versus 2.2 h). These results suggested that SiO_2 NP-triggered SIRT6 mRNA down-regulation is due to mRNA destabilization.

3.6. SIRT6 increases SiO_2 NP-induced ROS production

FST inhibits SiO_2 NP-induced ROS production. Since SIRT6 represses FST expression, we suspected that SIRT6 participates in SiO_2 NP-induced ROS production. We therefore overexpressed SIRT6 and detected cellular ROS level. Overexpression of SIRT6 significantly increased total ROS level in A549 cells. SIRT6 also increased SiO_2 NP-induced ROS production (Fig. 6A,B), indicating a promoting role of SIRT6 in ROS production.

3.7. SIRT6 promotes SiO_2 NP-induced cell apoptosis

SiO_2 NP treatment induces cellular toxicity (Kaewamatawong et al., 2006; Nel et al., 2006). We suspected that SIRT6 promoted cell apoptosis. We overexpressed SIRT6 and detected cell viability. Data showed significantly decreased cell viability in SIRT6-expressing cells compared to control cells after SiO_2 NP treatment (Fig. 7A). Annexin V staining showed similar result. The apoptotic cells were low in normal growth groups (4.4%) and SIRT6 overexpression did not induce cell apoptosis (4.3%). SiO_2 NP treatment for 12 h induced more cell apoptosis in SIRT6-expressing group (14.1%) than control cells (5.0%) (Fig. 7B), indicating that SIRT6 promotes SiO_2 NP-induced cell apoptosis. The data was further confirmed by more caspase3 cleavage in SIRT6-expressing group than control cells after SiO_2 NP treatment (Fig. 7C).

4. Discussion

We have previously reported the up-regulation of FST triggered by SiO_2 NP stress, which performs a protective role (Lin et al., 2016). However, the detailed mechanism is unknown. In this study, we demonstrated SIRT6 as a negative regulator of FST expression. Chromatin immunoprecipitation studies revealed a direct binding of SIRT6 with FST promoter. SiO_2 NP treatment represses the expression of SIRT6, and thus activates the transcription of FST. Our data provided direct evidence that silica nanoparticle up-regulates FST transcription through releasing SIRT6-induced epigenetic silencing (Fig. 7D).

FST has been demonstrated as a stress responsive gene. The expression of FST is low under normal condition, while its expression is induced during stresses such as glucose deprivation or SiO_2 NP exposure. Stress-induced FST expression could be regulated at either transcriptional or post-transcriptional level. We have reported that FST mRNA bears a AU-rich element which mediates its decay under normal condition by AUF1. During energy deficiency stress, AUF1 is translocated from cytoplasm to nucleus, allowing a quick stabilization of FST mRNA and the up-regulation of FST protein (Gao et al., 2014). However, SiO_2 NP exposure does not affect FST mRNA stability but induces

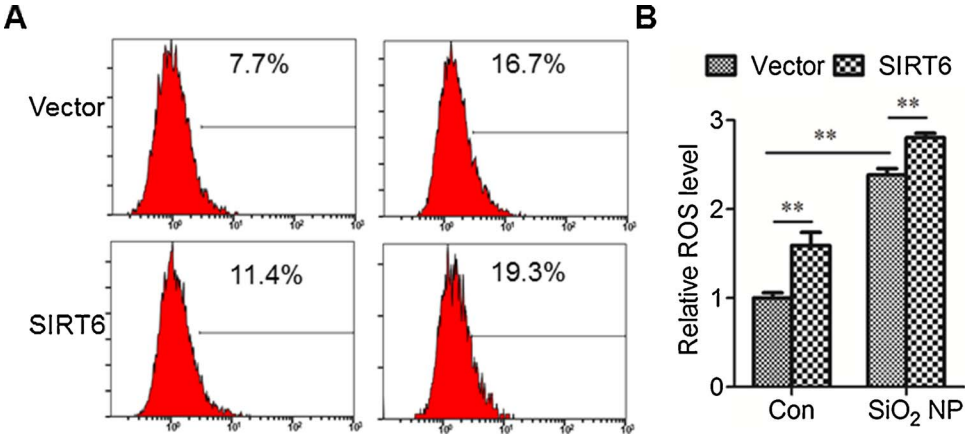

Fig. 6. SIRT6 increases SiO_2 NP-induced ROS production.
(A) A549 cells transfected with vector or SIRT6 gene were treated with or without 50 μg/mL of SiO_2 NPs for 2 h. Intracellular ROS level was detected by DCFH-DA fluorescent probe and flow cytometry. (B) Relative ROS level was calculated. The values are the mean ± SD of three independent experiments. $^{**}P < 0.01$.

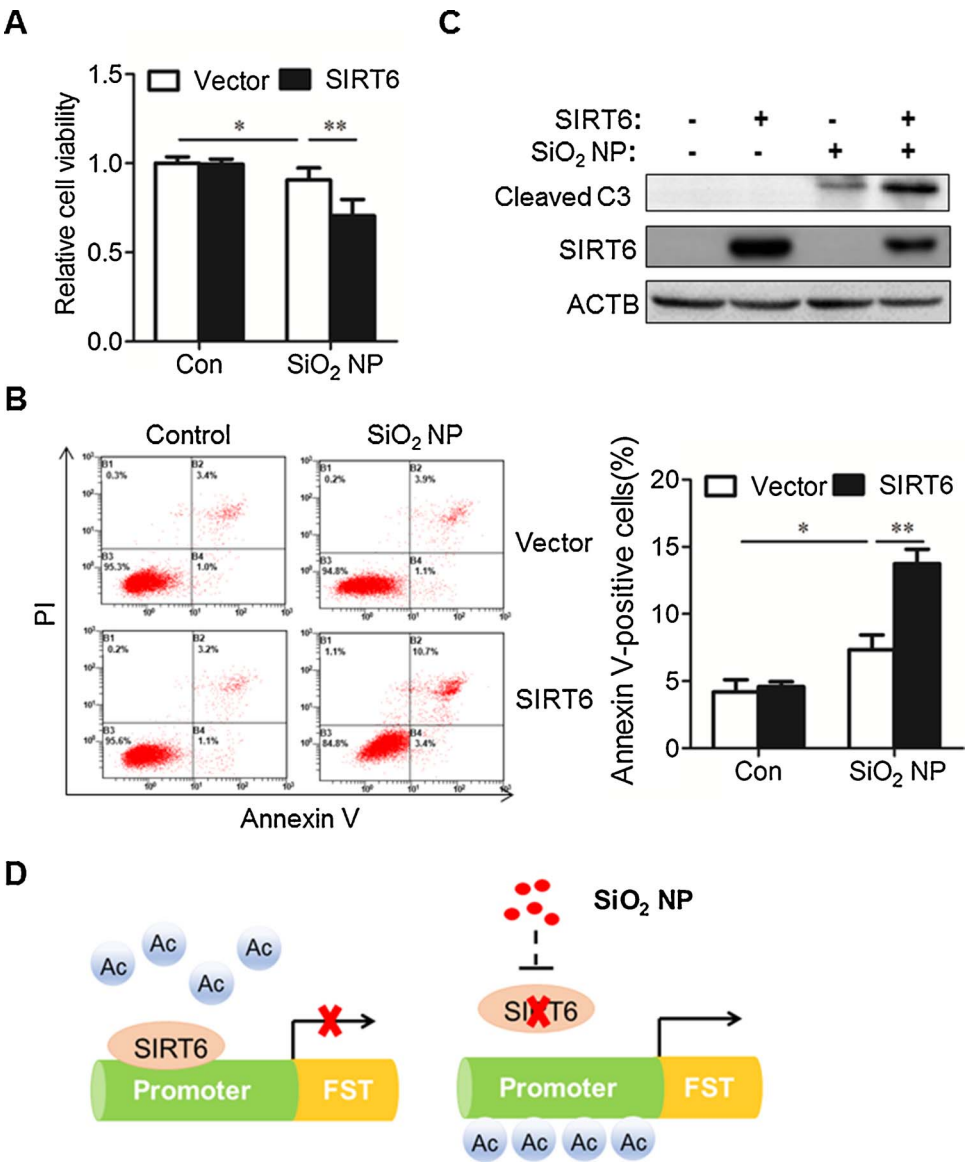

Fig. 7. SIRT6 promotes SiO_2 NP-induced cell apoptosis.
A549 cells transfected with plasmid expressing SIRT6 or control vector were treated with or without 50 μg/mL of SiO_2 NPs for 12 h. (A) Cell viability was determined using cell counting kit-8 (CCK-8). (B) Cell apoptosis was monitored by annexin V-FITC staining and flow cytometry analysis. Annexin-V positive cells were quantified. The values are the mean ± SD of three independent experiments. $^*P < 0.05$, $^{**}P < 0.01$. (C) Cleaved caspase3 (Cleaved C3) was detected by immunoblotting. (D) Schematic model for SIRT6-regulated FST expression during SiO_2 NP treatment. Under normal condition, SIRT6 binds to FST promoter and induces FST gene silencing. SiO_2 NP reduces SIRT6 expression, leading to the transcription of FST gene.

FST gene transcription. We have identified transcription factor Nrf2 mediating FST transcription during SiO_2 NP treatment (Lin et al., 2016). In this report, we identified SIRT6 as a negative regulator of FST transcription. SIRT6 de-acetylates H3K9 and H3K56 level at FST promoter region, which induces FST gene silencing under normal condition. SiO_2 NP exposure decreases SIRT6 expression, which loosens FST chromatin and activates FST gene transcription. Our data showed that SIRT1 also repressed FST expression. However, SIRT1 did not bind to FST promoter, suggesting that SIRT1 regulates FST expression through other factors. Interestingly, our data showed that SIRT1 could positively regulate SIRT6 expression (Fig. S4), which was also reported by other group (Kim et al., 2010). These data strongly suggested that SIRT1 repressed FST expression through up-regulating SIRT6 level.

SIRT6 acts as a co-repressor of the transcription factors. Therefore, SIRT6 binds its target genes through its interacting transcription factors. For example, SIRT6 negatively regulates NF-κB dependent transcription via histone H3K9 deacetylation (Kawahara et al., 2009). Besides, SIRT6 functions as a histone H3K9 deacetylase to control the expression of multiple glycolytic genes, which mediates co-repressing Hif1α transcriptional activity and contributes to glucose homeostasis (Zhong et al., 2010). Study has also demonstrated that SIRT6 controls cancer cell metabolism by co-repressing Myc transcriptional activity (Kugel et al., 2016; Sebastian et al., 2012). How SIRT6 is recruited to FST promoter and which factors mediates this process need to be further studied.

SIRT6 is involved in cellular stress responses including DNA damage response and oxidative stress response (Mao et al., 2011; Pan et al., 2016; Rizzo et al., 2017). Based on the critical role of SIRT6, its expression is tightly controlled under stresses. Our data showed reduced expression of SIRT6 during SiO_2 NP exposure. Other studies have also demonstrated that SIRT6 levels are down-regulated under various stressful conditions such as cellular senescence, oxygen and glucose deprivation, or oxidative stress triggered by H_2O_2 (Lee et al., 2013; Liu et al., 2014; Shao et al., 2016; Takasaka et al., 2014). However, the detailed regulatory mechanism remains elusive. Our present data showed that SiO_2 NP treatment significantly reduced the half-life of SIRT6 mRNA without affecting SIRT6 promoter activity, indicating a post-transcriptional regulatory mechanism. It has been reported that several microRNAs target SIRT6, including miR-33b, miR-34a, miR-122 and miR-766 (Baker et al., 2016; Davalos et al., 2011; Elhanati et al., 2016; Lefort et al., 2013; Sharma et al., 2013). The interaction between these microRNAs with SIRT6 mRNA might explain SiO_2 NP-mediated SIRT6 mRNA decay.

In summary, we have identified SIRT6 as a negative regulator of FST

which participates in SiO_2 NP toxicity. These findings uncover a new mechanism of FST expression regulation during stresses.

Acknowledgements

This work was supported by grants from National Natural Science Foundation of China (81472563, 81672847 to X.G., and 31600630 to H.D.), and the Fundamental Research Funds for the Central Universities (2017QNA7021 to X.G.).

Appendix A. Supplementary data

Supplementary data associated with this article can be found, in the online version, at https://doi.org/10.1016/j.biocel.2017.12.011.

References

Amthor, H., Nicholas, G., McKinnell, I., Kemp, C.F., Sharma, M., Kambadur, R., Patel, K., 2004. Follistatin complexes Myostatin and antagonises Myostatin-mediated inhibition of myogenesis. Dev. Biol. 270 (1), 19–30.

Baker, J.R., Vuppusetty, C., Colley, T., Papaioannou, A.I., Fenwick, P., Donnelly, L., Ito, K., Barnes, P.J., 2016. Oxidative stress dependent microRNA-34a activation via PI3Kalpha reduces the expression of sirtuin-1 and sirtuin-6 in epithelial cells. Sci. Rep. 6, 35871.

Brown, D.M., Kanase, N., Gaiser, B., Johnston, H., Stone, V., 2014. Inflammation and gene expression in the rat lung after instillation of silica nanoparticles: effect of size, dispersion medium and particle surface charge. Toxicol. Lett. 224 (1), 147–156.

Davalos, A., Goedeke, L., Smibert, P., Ramirez, C.M., Warrier, N.P., Andreo, U., Cirera-Salinas, D., Rayner, K., Suresh, U., Pastor-Pareja, J.C., Esplugues, E., Fisher, E.A., Penalva, L.O., Moore, K.J., Suarez, Y., Lai, E.C., Fernandez-Hernando, C., 2011. miR-33a/b contribute to the regulation of fatty acid metabolism and insulin signaling. Proc. Natl. Acad. Sci. U. S. A. 108 (22), 9232–9237.

Elhanati, S., Ben-Hamo, R., Kanfi, Y., Varvak, A., Glazz, R., Lerrer, B., Efroni, S., Cohen, H.Y., 2016. Reciprocal regulation between SIRT6 and miR-122 controls liver metabolism and predicts hepatocarcinoma prognosis. Cell Rep. 14 (2), 234–242.

Gao, X., Dong, H., Lin, C., Sheng, J., Zhang, F., Su, J., Xu, Z., 2014. Reduction of AUF1-mediated follistatin mRNA decay during glucose starvation protects cells from apoptosis. Nucleic Acids Res. 42 (16), 10720–10730.

Glister, C., Kemp, C.F., Knight, P.G., 2004. Bone morphogenetic protein (BMP) ligands and receptors in bovine ovarian follicle cells: actions of BMP-4, −6 and −7 on granulosa cells and differential modulation of Smad-1 phosphorylation by follistatin. Reproduction 127 (2), 239–254.

Hemmati-Brivanlou, A., Kelly, O.G., Melton, D.A., 1994. Follistatin, an antagonist of activin, is expressed in the Spemann organizer and displays direct neuralizing activity. Cell 77 (2), 283–295.

Jiang, M., Ku, W.Y., Zhou, Z., Dellon, E.S., Falk, G.W., Nakagawa, H., Wang, M.L., Liu, K., Wang, J., Katzka, D.A., Peters, J.H., Lan, X., Que, J., 2015. BMP-driven NRF2 activation in esophageal basal cell differentiation and eosinophilic esophagitis. J. Clin. Invest. 125 (4), 1557–1568.

Kaewamatawong, T., Shimada, A., Okajima, M., Inoue, H., Morita, T., Inoue, K., Takano, H., 2006. Acute and subacute pulmonary toxicity of low dose of ultrafine colloidal silica particles in mice after intratracheal instillation. Toxicol. Pathol. 34 (7), 958–965.

Kawahara, T.L., Michishita, E., Adler, A.S., Damian, M., Berber, E., Lin, M., McCord, R.A., Ongaigui, K.C., Boxer, L.D., Chang, H.Y., Chua, K.F., 2009. SIRT6 links histone H3 lysine 9 deacetylation to NF-kappaB-dependent gene expression and organismal life span. Cell 136 (1), 62–74.

Kim, H.S., Xiao, C., Wang, R.H., Lahusen, T., Xu, X., Vassilopoulos, A., Vazquez-Ortiz, G., Jeong, W.I., Park, O., Ki, S.H., Gao, B., Deng, C.X., 2010. Hepatic-specific disruption of SIRT6 in mice results in fatty liver formation due to enhanced glycolysis and triglyceride synthesis. Cell Metab. 12 (3), 224–236.

Kugel, S., Sebastian, C., Fitamant, J., Ross, K.N., Saha, S.K., Jain, E., Gladden, A., Arora, K.S., Kato, Y., Rivera, M.N., Ramaswamy, S., Sadreyev, R.I., Goren, A., Deshpande, V., Bardeesy, N., Mostoslavsky, R., 2016. SIRT6 suppresses pancreatic cancer through control of lin28b. Cell 165 (6), 1401–1415.

Lee, O.H., Kim, J., Kim, J.M., Lee, H., Kim, E.H., Bae, S.K., Choi, Y., Nam, H.S., Heo, J.H., 2013. Decreased expression of sirtuin 6 is associated with release of high mobility group box-1 after cerebral ischemia. Biochem. Biophys. Res. Commun. 438 (2), 388–394.

Lefort, K., Brooks, Y., Ostano, P., Cario-Andre, M., Calpini, V., Guinea-Viniegra, J., Albinger-Hegyi, A., Hoetzenecker, W., Kolfschoten, I., Wagner, E.F., Werner, S., Dotto, G.P., 2013. A miR-34a-SIRT6 axis in the squamous cell differentiation network. EMBO J. 32 (16), 2248–2263.

Li, Z., Barnes, J.C., Bosoy, A., Stoddart, J.F., Zink, J.I., 2012. Mesoporous silica nanoparticles in biomedical applications. Chem. Soc. Rev. 41 (7), 2590–2605.

Lim, R., Acharya, R., Delpachitra, P., Hobson, S., Sobey, C.G., Drummond, G.R., Wallace, E.M., 2015. Activin and NADPH-oxidase in preeclampsia: insights from in vitro and murine studies. Am. J. Obstet. Gynecol. 212 (1) (86 e81-12).

Lin, C., Zhao, X., Sun, D., Zhang, L., Fang, W., Zhu, T., Wang, Q., Liu, B., Wei, S., Chen, G., Xu, Z., Gao, X., 2016. Transcriptional activation of follistatin by Nrf2 protects pulmonary epithelial cells against silica nanoparticle-induced oxidative stress. Sci. Rep. 6, 21133.

Liu, R., Liu, H., Ha, Y., Tilton, R.G., Zhang, W., 2014. Oxidative stress induces endothelial cell senescence via downregulation of Sirt6. BioMed Res. Int. 2014, 902842.

Livak, K.J., Schmittgen, T.D., 2001. Analysis of relative gene expression data using real-time quantitative PCR and the 2(-Delta Delta C(T)) Method. Methods 25 (4), 402–408.

Ma, Q., 2013. Role of nrf2 in oxidative stress and toxicity. Annu. Rev. Pharmacool. Toxicol. 53, 401–426.

Mao, Z., Hine, C., Tian, X., Van Meter, M., Au, M., Vaidya, A., Seluanov, A., Gorbunova, V., 2011. SIRT6 promotes DNA repair under stress by activating PARP1. Science 332 (6036), 1443–1446.

Michishita, E., Park, J.Y., Burneskis, J.M., Barrett, J.C., Horikawa, I., 2005. Evolutionarily conserved and nonconserved cellular localizations and functions of human SIRT proteins. Mol. Biol. Cell 16 (10), 4623–4635.

Michishita, E., McCord, R.A., Berber, E., Kioi, M., Padilla-Nash, H., Damian, M., Cheung, P., Kusumoto, R., Kawahara, T.L., Barrett, J.C., Chang, H.Y., Bohr, V.A., Ried, T., Gozani, O., Chua, K.F., 2008. SIRT6 is a histone H3 lysine 9 deacetylase that modulates telomeric chromatin. Nature 452 (7186), 492–496.

Michishita, E., McCord, R.A., Boxer, L.D., Barber, M.F., Hong, T., Gozani, O., Chua, K.F., 2009. Cell cycle-dependent deacetylation of telomeric histone H3 lysine K56 by human SIRT6. ABBV Cell Cycle 8 (16), 2664–2666.

Nakamura, T., Takio, K., Eto, Y., Shibai, H., Titani, K., Sugino, H., 1990. Activin-binding protein from rat ovary is follistatin. Science 247 (4944), 836–838.

Nel, A., Xia, T., Madler, L., Li, N., 2006. Toxic potential of materials at the nanolevel. Science 311 (5761), 622–627.

Nel, A.E., Madler, L., Velegol, D., Xia, T., Hoek, E.M., Somasundaran, P., Klaessig, F., Castranova, V., Thompson, M., 2009. Understanding biophysicochemical interactions at the nano-bio interface. Nat. Mater. 8 (7), 543–557.

Oberdorster, G., 2010. Safety assessment for nanotechnology and nanomedicine: concepts of nanotoxicology. J. Intern. Med. 267 (1), 89–105.

Pan, H., Guan, D., Liu, X., Li, J., Wang, L., Wu, J., Zhou, J., Zhang, W., Ren, R., Li, Y., Yang, J., Hao, Y., Yuan, T., Yuan, G., Wang, H., Ju, Z., Mao, Z., Qu, J., Tang, F., Liu, G.H., 2016. SIRT6 safeguards human mesenchymal stem cells from oxidative stress by coactivating NRF2. Cell Res. 26 (2), 190–205.

Parenti, M.D., Grozio, A., Bauer, I., Galeno, L., Damonte, P., Millo, E., Sociali, G., Franceschi, C., Ballestrero, A., Bruzzone, S., Del Rio, A., Nencioni, A., 2014. Discovery of novel and selective SIRT6 inhibitors. J. Med. Chem. 57 (11), 4796–4804.

Rizzo, A., Iachettini, S., Salvati, E., Zizza, P., Maresca, C., D'Angelo, C., Benarroch-Popivker, D., Capolupo, A., Del Gaudio, F., Cosconati, S., Di Maro, S., Merlino, F., Novellino, E., Amoreo, C.A., Mottolese, M., Sperduti, I., Gilson, E., Biroccio, A., 2017. SIRT6 interacts with TRF2 and promotes its degradation in response to DNA damage. Nucleic Acids Res. 45 (4), 1820–1834.

Sebastian, C., Zwaans, B.M., Silberman, D.M., Gymrek, M., Goren, A., Zhong, L., Ram, O., Truelove, J., Guimaraes, A.R., Toiber, D., Cosentino, C., Greenson, J.K., MacDonald, A.I., McGlynn, L., Maxwell, F., Edwards, J., Giacosa, S., Guccione, E., Weissleder, R., Bernstein, B.E., Regev, A., Shiels, P.G., Lombard, D.B., Mostoslavsky, R., 2012. The histone deacetylase SIRT6 is a tumor suppressor that controls cancer metabolism. Cell 151 (6), 1185–1199.

Shao, J., Yang, X., Liu, T., Zhang, T., Xie, Q.R., Xia, W., 2016. Autophagy induction by SIRT6 is involved in oxidative stress-induced neuronal damage. Protein Cell 7 (4), 281–290.

Sharma, A., Diecke, S., Zhang, W.Y., Lan, F., He, C., Mordwinkin, N.M., Chua, K.F., Wu, J.C., 2013. The role of SIRT6 protein in aging and reprogramming of human induced pluripotent stem cells. J. Biol. Chem. 288 (25), 18439–18447.

Takasaka, N., Araya, J., Hara, H., Ito, S., Kobayashi, K., Kurita, Y., Wakui, H., Yoshii, Y., Yumino, Y., Fujii, S., Minagawa, S., Tsurushige, C., Kojima, J., Numata, T., Shimizu, K., Kawaishi, M., Kaneko, Y., Kamiya, N., Hirano, J., Odaka, M., Morikawa, T., Nishimura, S.L., Nakayama, K., Kuwano, K., 2014. Autophagy induction by SIRT6 through attenuation of insulin-like growth factor signaling is involved in the regulation of human bronchial epithelial cell senescence. J. Immunol. 192 (3), 958–968.

Tasselli, L., Xi, Y., Zheng, W., Tennen, R.I., Odrowaz, Z., Simeoni, F., Li, W., Chua, K.F., 2016. SIRT6 deacetylates H3K18ac at pericentric chromatin to prevent mitotic errors and cellular senescence. Nat. Struct. Mol. Biol. 23 (5), 434–440.

Yang, B., Zwaans, B.M., Eckersdorff, M., Lombard, D.B., 2009. The sirtuin SIRT6 deacetylates H3 K56Ac in vivo to promote genomic stability. ABBV Cell Cycle 8 (16), 2662–2663.

Zhong, L., D'Urso, A., Toiber, D., Sebastian, C., Henry, R.E., Vadysirisack, D.D., Guimaraes, A., Marinelli, B., Wikstrom, J.D., Nir, T., Clish, C.B., Vaitheesvaran, B., Iliopoulos, O., Kurland, I., Dor, Y., Weissleder, R., Shirihai, O.S., Ellisen, L.W., Espinosa, J.M., Mostoslavsky, R., 2010. The histone deacetylase Sirt6 regulates glucose homeostasis via Hif1alpha. Cell 140 (2), 280–293.